PRACTICAL EVALUATIONS OF PARASITIC RESONANT PWM DC-DC CONVERTERS FOR HIGH-POWER MEDICAL USE

H. Takano and J. Takahashi
Research and Development Center Hitachi Medical
Corporation, 2-1, Shintoyofuta, Kashiwa, Chiba,
277-0804, Japan

J. M. Sun, L..Gamage and M. Nakaoka
The Graduate School of Engineering and
Science,Yamaguchi University, 2557, Tokiwadai, Ube,
755-8611, Japan

ABSTRACT This paper presents a novel non-reso-
nant PWM DC-DC converter for X-ray high-voltage power
generator using the parasitic impedances of the high-volt-
age high-frequency link transformer with its output high-
voltage control scheme and steady-state characteristics
compared to the conventional series-parallel resonant DC-
DC converter. The key point of this approach is to evaluate
effectiveness of reduction of the turn ratio of the high-volt-
age high-frequency transformer on improvements in power
conversion efficiency and the power factor applying a boost
AC-DC converter as DC voltage source, especially in the
long exposure term and light output load ranges.

1. INTRODUCTION

Recently, a variety of power applications of resonant in-
verter type DC-DC power converters with a high-frequency
transformer link have been studied [1]-[3]. The series-par-
allel resonant DC-DC converter is suitable for high-power
X-ray generators because of its adaptability to their ex-
tremely wide output power and load ranges in medical use.

In the high-voltage high-frequency application, the elec-
tromagnetic coupling coefficient of the primary and the sec-
ondary windings of the transformer is not so high and the
parasitic leakage inductance is apt to be large because of its
large turn ratio and allowable insulation [6][7]. According
to the increase of the inverter operating frequency, the leak-
age inductance of the high-voltage high-frequency trans-
former makes enlarge the impedance in the inverter load
circuitry. This enlarged impedance limits the inverter out-
put current and the output DC current, tube current. In order
to compensate the enlarged impedance and to obtain high
output power, the series resonant topology have been intro-
duced with a resonant capacitance connected in series to the
leakage inductance.

Moreover, the secondary-side equivalent stray lumped
capacitance is not negligible. This secondary-side stray ca-
pacitance is useful for regulation of the output DC voltage
as a parallel resonant capacitance as well as the series reso-
nant capacitance.

However, because of ineffective current flowing the sec-
ondary-side stray capacitance, the total power conversion

efficiency is decreased comparatively with the losses
caused by the secondary-side stray capacitance.

Nevertheless, for the moment, improvement on the total
power conversion efficiency and the AC input power factor
of the medical-use X-ray high-voltage generators have not
been sufficiently discussed and considered from the power
conversion topologies and their control strategies.

This paper presents the newly developed non-resonant
PWM DC-DC converter for X-ray high-voltage power gen-
erator employing the parasitic impedances of the high-volt-
age high-frequency link transformer and its output high-
voltage control scheme as well as steady-state characteris-
tics compared to the conventional series-parallel resonant
DC-DC converter.

The purpose of this approach is to improve power conver-
sion efficiency and the power factor according to a reduc-
tion of the turn ratio of the high-voltage high-frequency
transformer on by use of a boost AC-DC converter as DC
voltage source, especially, in the long exposure term and
light output load ranges.

2. NOVEL NON-RESONANT PWM INVERTER-FED DC-DC CONVERTER TYPE X-RAY POWER GENERATOR

Fig. 1 illustrates the newly developed non-resonant PWM
inverter-fed DC-DC converter designed for 32-kW class X-
ray power generator. The solid-state X-ray high-voltage
power generator using high-frequency IGBTs inverter men-
tioned above consists of a single-phase high-power factor
hybrid bridge boost AC-DC converter, a non-resonant
PWM inverter, a high-voltage high-frequency link trans-
former, a high-voltage rectifier connected to a pair of high-
voltage feeding cables and an X-ray tube as a load. The
high-power factor boost AC-DC converter consists of two
IGBTs (1200V/300A), two high-speed soft-recovery di-
odes, an AC reactor and so on.

The features of this X-ray power generator are to use the
parasitic lumped leakage-inductance and the secondary-
side lumped stray capacitance of the high-voltage high-fre-

C_p^* : Stray capacitance of HV transformer
(secondary-side value)
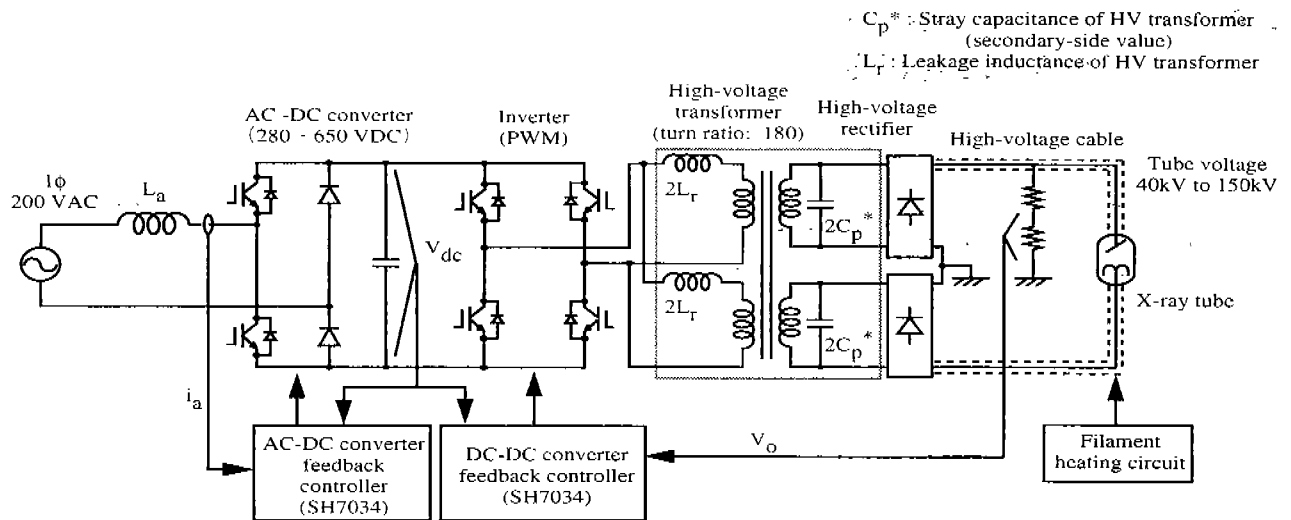L_r : Leakage inductance of HV transformer

Fig. 1. Schematic configuration of newly developed non-resonant PWM inverter-fed DC-DC converter with single phase high-power factor boost AC-DC converter designed for 32-kW class X-ray power generator.

quency transformer to regulate output voltage applying PWM operation of the non-resonant inverter. In addition to this, the input-side equivalent capacitance of the high-voltage cables are effectively used as the output smoothing DC filter. The inverter switching frequency is 20 kHz constant and the AC-DC converter switching frequency is 15.6 kHz.

The X-ray tube load can be electrically modeled as a variable load resistance circuitry which is determined according to the precise regulation of the filament heating current in the cathode of X-ray tube. Its filament current can be continuously regulated by the another resonant inverter with a high-frequency transformer isolated link.

The other remarkable feature of this non-resonant PWM inverter-fed X-ray generator is to be introduced a single-phase high-power factor boost AC-DC converter in order to obtain higher DC link voltage from 280 V to 650 V than the DC link voltage of the conventional series-parallel resonant DC-DC converter described later. Therefore, the turn ratio of the high-voltage high-frequency transformer is much smaller than the conventional DC-DC converter, in this case, the turn ratio is 180. The DC link voltage V_{dc} is optimized to adopt the extremely wide load range for medical use high-voltage applications.

3. SERIES-PARALLEL RESONANT INVERTER-FED DC-DC CONVERTER TYPE X-RAY POWER GENERATOR

Fig. 2 illustrates the conventional series-parallel resonant inverter-fed DC-DC converter type 50-kW class X-ray generator developed by the authors . This X-ray generator consists of a single-phase thyristor bridge voltage doubler rectifier to obtain higher DC voltage source than full bridge type rectifiers, a fixed frequency phase-shifted PWM control-

based high-frequency resonant inverter with a high-voltage high-frequency transformer link, a high-voltage diode rectifier connected into the high-voltage cables, and an X-ray tube as a load of this resonant DC-DC converter.

The features of this type of X-ray power generator are to make the most of the parasitic lumped leakage-inductance and the secondary-side lumped parallel capacitance of the high-voltage high-frequency transformer as the LC resonant circuit components in addition to the input-side equivalent capacitance of the high-voltage DC cables as the output smoothing DC filter. The series resonant capacitor only is to be externally connected to the primary-side of the high-voltage high-frequency transformer. These parasitic circuit parameters of are also utilized to regulate output DC high-voltage together with the phase-shift PWM technique.

The high-voltage link transformer of this X-ray high-voltage power generator has a larger turn ratio 490, in this case, than the non-resonant DC-DC type presented in Fig. 1.

4. HIGH-VOLTAGE HIGH-FREQUENCY TRANSFORMER

A. Structure and Features

Fig. 3 illustrates the high-voltage high-frequency transformer designed newly for non-resonant PWM high-frequency link. Although the conventional high-voltage link transformer for the X-ray generator has a large turn ratio; about 400 to 500 in the conventional design so as to obtain the high-voltage DC up to 150 kV from 200 V or 400 V AC line, the smaller turn ratio; 180 is chosen here in addition to applying the boost AC-DC converter.

As the primary windings, Litz wire is coiled to a pair of bobbins for two legs in a single layer. The secondary wind-

C_s : Series compensated capacitor
C_p^* : Stray capacitance of HV transformer
(secondary-side value)
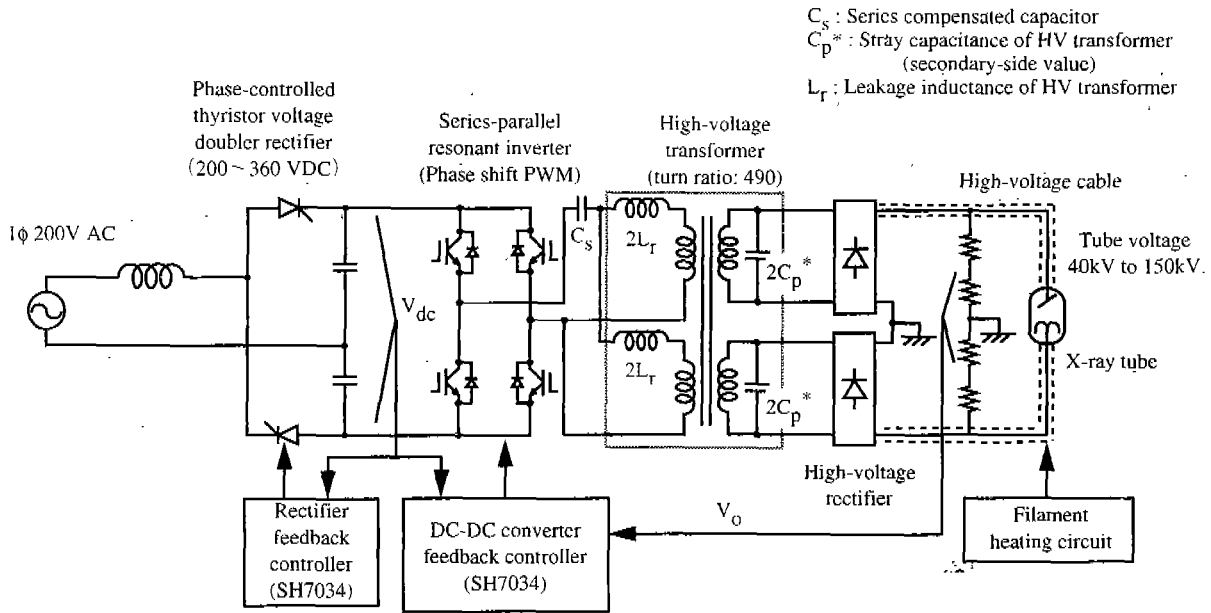L_r : Leakage inductance of HV transformer

Fig. 2. Conventional series-parallel resonant phase-shift PWM inverter-fed DC-DC converter with thyristor voltage doubler rectifier designed for 50-kW class X-ray power generator.

ings are separated into four blocks and coiled in dozens of layers on the primary windings.

Moreover, FINEMET® (Hitachi Metals Ltd.) is introduced as iron core material in place of the conventional ferrite core applying its features of high saturation magnetic flux density in order to reduce the leakage inductance and the stray capacitance in consequence of the smaller core cross section in addition to its low iron loss property.

B. Leakage Inductance

Sufficient isolated distance between the primary and the secondary-windings is practically required to obtain the allowable insulation voltage. Therefore, the electromagnetic coupling coefficient of the primary and the secondary windings of the high-voltage high-frequency transformer is not so high and the parasitic leakage inductance is apt to be large.

According to the increase of the inverter operating frequency, the leakage inductance of the high-voltage high-frequency transformer makes enlarge the impedance in the inverter load circuitry and limits the inverter output current and the X-ray tube current. Therefore, in the conventional series-parallel resonant DC-DC converter, the leakage inductance is compensated by the series resonant capacitance.

This leakage-inductances can be approximately treated as the lumped series resonant inductance L_r and estimated as follows;

$$L_r = \frac{k\,\pi\,N_1^2(u_1 + u_2)}{h_1}\left(\frac{\delta_1 + \delta_2}{3} + \delta_0\right) \times 10^{-7} \quad (1)$$

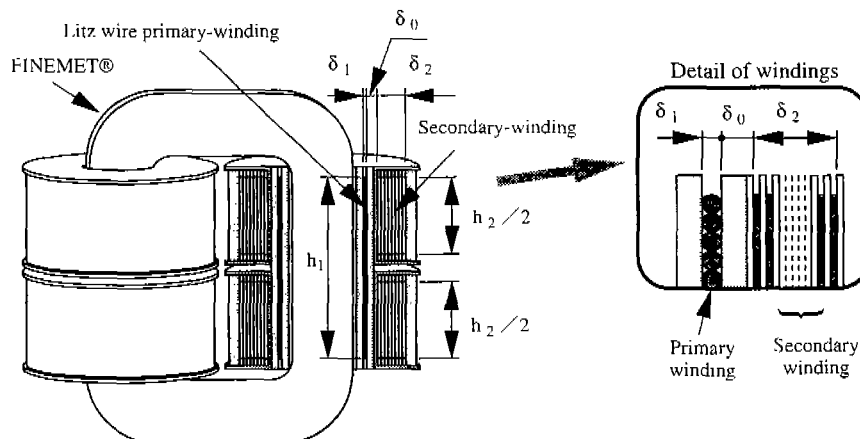$$k = 1 - \frac{1}{\pi}\frac{\delta_0 + \delta_1 + \delta_2}{h_1} \quad (2)$$

Fig. 3 Newly designed high-voltage transformer using FINEMET® iron core.

where, L_r : the leakage inductance reduced into the primary-side port (H) ; k : Rogowski's correction coefficient ; N_1 : the turn number of the primary winding; u_1 and u_2 : the average one turn lengths of the primary and the secondary windings (m) ; h_1, δ_0 , δ_1 and δ_2 : the geometric dimensions of the high-voltage transformer shown in Fig. 3.

Equ. 1 indicates the leakage indicates Lr is proportional to square of the turn number N_1. Consequently, smaller turn number of the primary windings is very effective to decrease the inverter load circuitry impedance.

C. Stray Capacitance of The Secondary-side Windings

The stray capacitances exist mainly between respective layers so that the secondary windings coiled in dozens of layers and isolated from one another with oil immersed papers. These distributed stray-capacitances are also treated here as a lumped stray-capacitance C_p reduced value into the primary side. The stray capacitance is connected in parallel to the load and is not negligible so that its primary side value reduced multiplying by square of the large turn ratio is considerably large. Extremely small stray capacitance increases the resonant frequency of the inverter resonant tank in the light load conditions and makes difficult to control the tube voltage. Therefore, in order to obtain rapid and stable tube voltage waveforms, the authors set the stray capacitance a third of the series compensated resonant capacitance in the conventional series-parallel resonant DC-DC converter.

The lumped stray-capacitance of the high-voltage high-frequency transformer is theoretically estimated by.

$$C_p = \frac{8 \pi \varepsilon_e \varepsilon_0 r_2 h_2 n^2}{3 d \left(m_{Layer} - 1\right) m_{2nd}^2 m_{Leg}}.$$ (3)

C_p : the lumped stray-capacitance of the high-voltage transformer reduced into the primary-side port (F) ; ε_0 : the dielectric constant of vacuum (F/m) ; ε_e : the equivalent relative dielectric constant of the oil immersed paper; n : the turn ratio of the high-voltage high-frequency transformer; r_2: the average radius of the secondary-side windings (m) ; h_2 : the effective height of the primary and the secondary windings (m) ; d : the distance between the two layers of the secondary windings (m) ; m Layer : the layer number of the secondary windings; m_{2nd} : the division number of the secondary windings for each leg; m_{Leg} : the number of the legs.

Equ. 3 means that the stray capacitance C_p is proportional to square of the turn ratio n. Consequently, lower turn ratio is significantly adequate to decrease the ineffective current flowing through the stray capacitance and inverter load current.

D. Consideration for Power Conversion Losses

As described later, the power losses of the high-voltage transformer ought to be represented using the equivalent resistances R_r, R_i corresponding to the iron and copper losses. The iron loss is proportional to the square of the applied effective voltage and the copper loss is determined by the effective current flowing through the primary and secondary windings of the high-voltage high-frequency transformer.

The stray capacitance ought to be reduced to decrease the ineffective current and the stray load loss of the high-voltage high-frequency transformer as well as conduction and switching losses of the inverter switches. In the series-parallel resonant DC-DC converter, however, the stray capacitance must be set desirable value, a third of the series capacitance, for the adequate tube voltage waveforms as described above. Consequently, it seems difficult to improve the total power conversion efficiency in the light load ranges under the limitations of the resonant operation which is advantageous for the high-power class X-ray generator.

As the another technique to improve the total power conversion efficiency, the non-resonant PWM inverter and the boost AC-DC converter so as to generate higher DC voltage source are introduced here in addition to the decrease of the turn ratio and together with the reduction of the stray capacitance of the high-voltage high-frequency transformer. As well known, the boost AC-DC converter can be also utilized to correct its power factor.
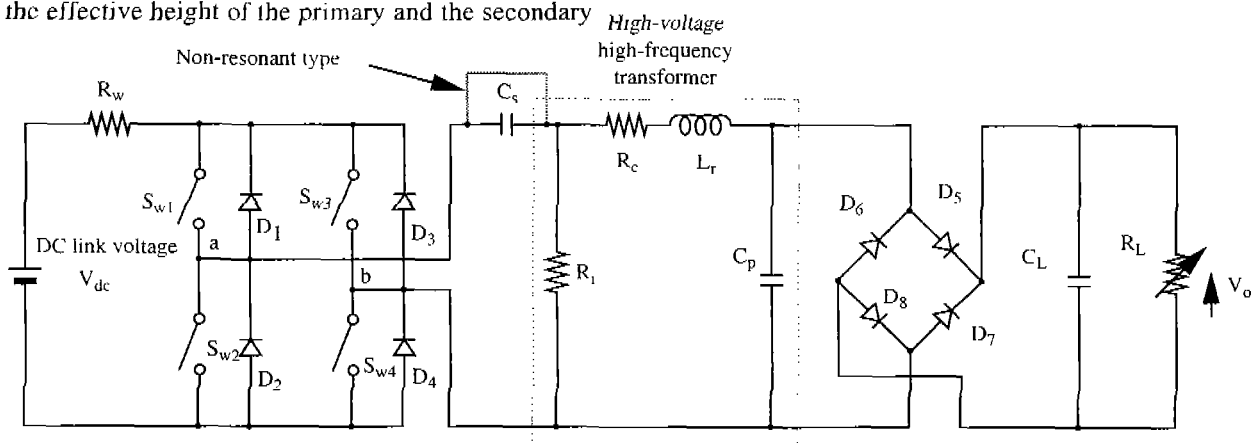

Fig. 4. Circuit model of non-resonant and series-parallel resonant DC-DC converter.

Table 1 Circuit parameters for simulation analysis.

Symbols	Items/Circuit topologies	Non-resonant	Series-Parallel
R_w	Lumped wiring resistance of main circuit (mΩ)	10	10
V_{dc}	DC link voltage (V)	650	360
L_r	Leakage inductance of high-voltage transformer (μH)	8.0	8.0
C_s	Series resonant capacitance (μF)	-	8.0
C_p	Stray capacitance of high-voltage transformer (μF)	0.6	2.7
C_L	Equivalent capacitance of high-voltage cable (μF)	42.1	310
R_L	Primary-side load resistance model of X-ray tube (Ω)	0.31 to 6200	0.04 to 830
$R_L{'}$	Secondary-side load resistance model of X-ray tube [MΩ]	0.01 to 200	0.01 to 200
R_i	Resistance corresponding to iron loss of high-voltage transformer (Ω)	385	280
R_c	Resistance corresponding to copper loss of high-voltage transformer (mΩ)	30	60
f_{inv}	Inverter frequency (kHz)	20	20
n	Turn ratio of high-voltage transformer	180	490

5. CIRCUIT SIMULATION AND CONTROL STRATEGY

ι. Circuit Model

Fig. 4 depicts the circuit model of non-resonant and se-ies-parallel resonant DC-DC converters for the X-ray high-oltage power generator. TABLE I indicates the circuit pa-ameters used for the simulation analysis. This circuit nodel is introduced under the following assumptions.

(1) The secondary-side load resistance $R_L{'}$ is estimated as he ratio of the tube voltage and the tube current,

(2) The input equivalent capacitances of the high-voltage .ables are utilized as the smoothing capacitor $C_L{'}$,

(3) The secondary-side value $R_L{'}$ and $C_L{'}$ are reduced nto its primary-side value R_L and C_L,

(4) The high-voltage transformer includes the leakage in-luctance L_r, the stray-capacitance C_p and the equivalent re-istances R_c, R_i represented by the lumped stray-load loss ιnd the equivalent iron loss.

(5) DC voltage source is modeled by V_{dc} instead of the)oost AC-DC converter. Besides, its impedance is pre-ιented by lumped wired resistance R_w.
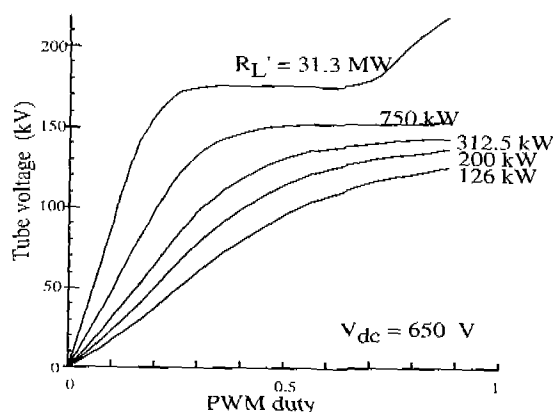
B. Simulated Load Ranges

Fig. 6 presents simulated steady-state characteristics of the non-resonant PWM DC-DC converter. This figure indi-cates the relations between PWM duty and the tube voltage for respective secondary side load resistances $R_L{'}$. These curves principally specified by the load resistances and the leakage inductance of the high-voltage high-frequency transformer. In case that PWM duty is more than 0.8 and the light load condition, $R_L{'}$=31.3 MΩ, the steady-state curve rises again against the PWM duty. The reason of this phenomena seems influence of the parallel resonance caused by the leakage inductance L_r and the stray-load ca-pacitance C_p.

Fig. 7 presents simulated steady-state characteristics of the series-parallel resonant phase-shift PWM DC-DC con-verter. The tube voltage can be regulated from zero to maxi-mum by the phase-shift angle as well as pulse width modu-lation in the non-resonant DC-DC converter. As well known, the phase-shift PWM technique is also feasible to control and compensate the impedance increase of the in-verter load circuitry in addition to the series-parallel reso-nant topology except some limitations of the impedance de-

Fig. 6. Simulated steady-state characteristics of non-resonant PWM DC-DC converter.
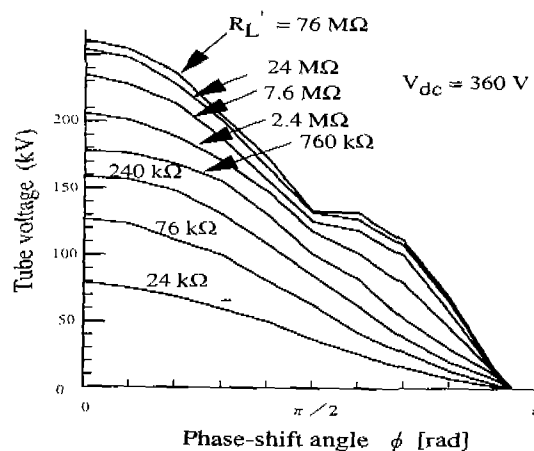

Fig. 7. Simulated steady-state characteristics of series-parallel resonant phase-shift PWM DC-DC converter.
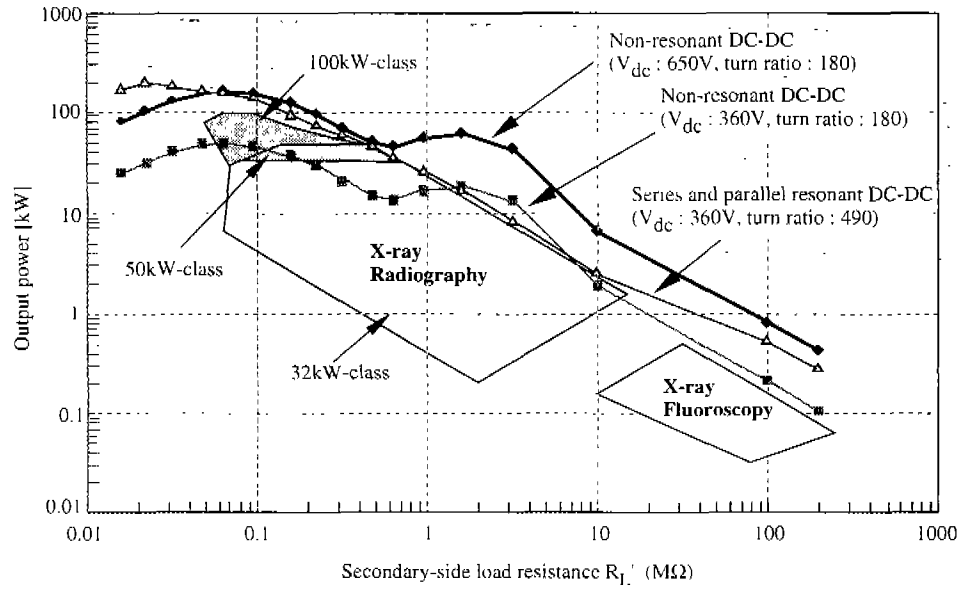
Fig. 8. Simulated output ranges for non-resonant topology and series-parallel resonant in the medical use X-ray generator.

sign of the resonant elements.

Fig. 8 presents the output power versus the load resistance characteristics as the simulated results under the comparison of the output load ranges in the actual medical-use X-ray high-voltage generator. There had been no way to obtain high-power X-ray using high-frequency inverter-fed DC-DC converter from 200 V AC input voltage because of the rather high impedance of the high-voltage high-fre-

quency transformer except using certain resonant topologies. And resonant topologies have a penalty of its low power conversion efficiency in the light load ranges. Although, Fig. 8 indicates the non-resonant DC-DC converter with boost converters might be able to obtain more than 100 kW high-voltage output power from 200 V AC input voltage.
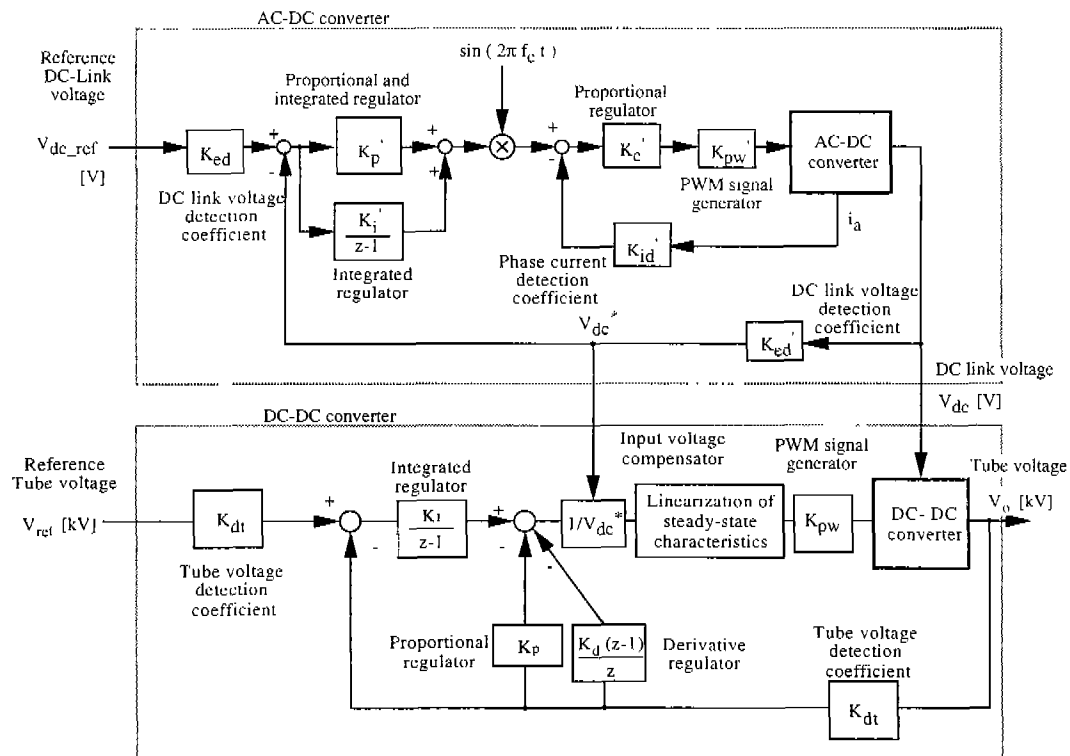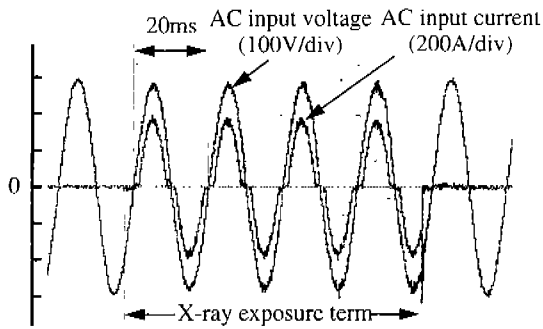

Fig. 9. Control block diagram for DC link voltage and tube voltage of non-resonant PWM DC-DC converter for X-ray generator.

20ms AC input voltage AC input current
(100V/div) (200A/div)

X-ray exposure term

AC input voltage : 207.0 Vrms (without exposure)
199.4 Vrms (during exposure)
AC input current : 218.5 Arms
Apparent power : 43.6 kVA
Power factor : 96.8 %

Fig. 10. Measured waveforms of AC input voltage and
AC input current.

C. Control Strategy

Fig. 9 illustrates the control block diagram of DC link
voltage and the tube voltage of the newly developed non-
resonant PWM DC-DC converter for X-ray generator intro-
ducing two 32-bit RISC (Reduced-instruction-set comput-
ing) processors SH7034 (Hitachi Ltd.). Roughly speaking,
this control system consists of two digital feedback control-
lers that is a PI controller for the single-phase boost AC-DC
high-power factor converter with P current minor loop and
I-PD controller for the non-resonant PWM DC-DC con-
verter with an input voltage fluctuation compensator and a
steady-state nonlinear characteristic compensator.

6. EXPERIMENTAL RESULTS AND DISCUSSIONS

Fig. 10 presents measured waveforms of the AC input
voltage and current waveforms. Due to the single-phase hy-
brid bridge boost AC-DC converter, the current distortions
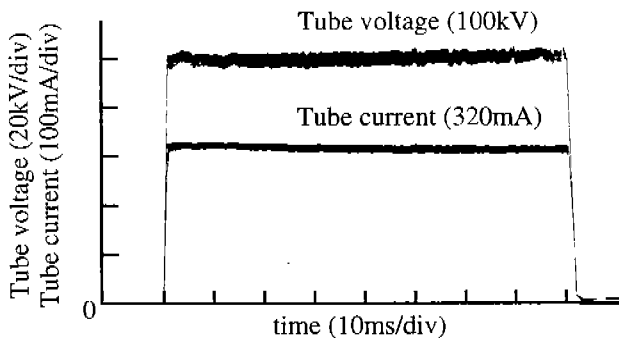are seen around zero current, however, the AC input current

Fig. 12. Measured tube voltage and tube current wave-
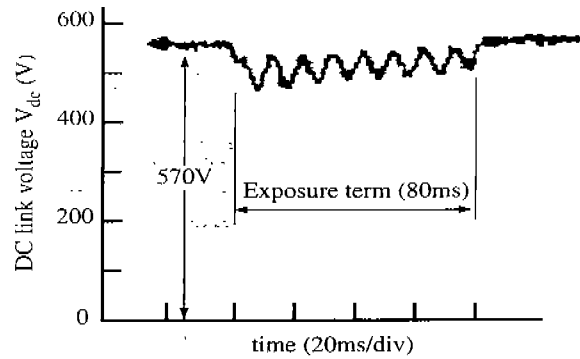forms of non-resonant DC-DC converter
(100 kV, 320 mA).

Fig. 11. Measured DC link voltage waveform of non-
resonant DC-DC converter (100 kV / 320 mA).

is almost sinusoidal and the power factor 96.8 % are accom-
plished in the maximum output power condition, 100 kV /
320 mA; the output power is 32 kW.

Fig. 11 shows measured DC link voltage waveform Vdc
of the non-resonant PWM DC-DC converter in the output
condition : 100 kV / 320 mA. The reference voltage
Vdc_ref is 570 V which is optimized to minimize power
loss of the non-resonant PWM inverter and its later cir-
cuitry. Around 80 V peak to peak fluctuation is seen in Vdc
during the X-ray exposure term. This voltage fluctuation
can be compensated by the input voltage fluctuation com-
pensator presented in Fig. 9.

Fig. 12 presents measured tube voltage and tube current
waveforms of non-resonant DC-DC converter type X-ray
generator in case of the maximum output condition, 100 kV
/ 320 mA, 32 kW. The voltage ripple is approximately 3 %.
The rise time is 0.6 ms; the fall time is 0.3 ms. Stable tube
voltage is obtained by digital feedback control shown in
Fig. 9.

Fig. 13 shows measured total power conversion effi-
ciency and power factor of non-resonant DC-DC converter
versus the output power. The power factor obtained by the
non-resonant DC-DC converter is extremely increased from
22 % of the series-parallel resonant DC-DC converter to 75
%. In case of the X-ray fluoroscopic load condition, 125 kV
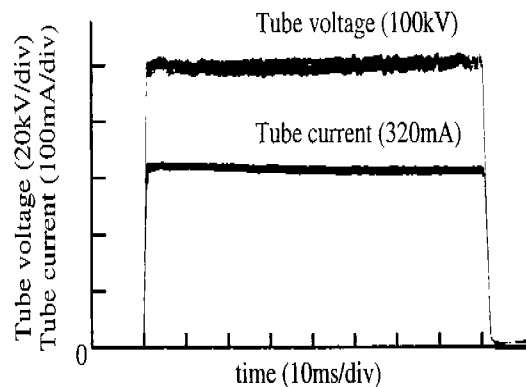/ 4 mA, the apparent power is reduced to more than a fifth.

Fig. 13. Measured total power conversion efficiency and
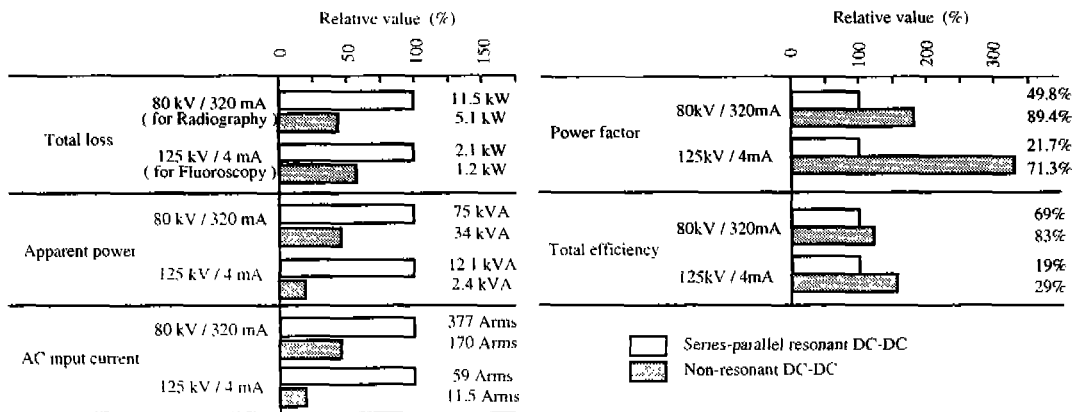power factor of non-resonant DC-DC converter.

Fig. 14. Comparison between series-parallel resonant and non-resonant DC-DC converters on measured loss, apparent power, AC input current, power factor and total efficiency.

The total power conversion efficiency is 75 % to 80 % in larger than 5 kW output power conditions. The power factor is grown from 62 % to 97 % according to the increase of the output power.

Fig. 14 represents comparisons of on measured power conversion total losses, apparent powers, AC input currents, power factors and total efficiencies for the non-resonant DC-DC converter type and the series-parallel resonant DC-DC type X-ray generators in the typical load conditions for the X-ray radiography, 80 kV / 320 mA, and for the X-ray fluoroscopy, 125 kV / 4 mA. The length of the bar charts indicates relative values to the series-parallel resonant DC-DC converter type X-ray generator. Effects of the reduction of the turn ration of the high-voltage high-frequency transformer and the decrease of the stray-capacitance introducing the single phase high-power factor boost AC/DC converter. These experimental results obviously prove that the ineffective current, main reason of the stray-load loss, flowing through stray capacitance of the high-voltage transformer is practically reduced and the total power conversion efficiency is improved by the proposed non-resonant PWM inverter-fed DC-DC converter for X-ray generator.

7. CONCLUSIONS

The novel non-resonant PWM DC-DC converter for X-ray high-voltage power generator using the parasitic impedances of the high-voltage high-frequency link transformer has been described comparing with the conventional series-parallel resonant DC-DC converter. The non-resonant PWM DC-DC converter with the boost converter might be able to obtain more than 100 kW high-voltage output power from 200 V AC input. Finally, as experimental results, effectiveness of reduction of the turn ratio of the high-voltage high-frequency transformer have been presented for improvements in the power conversion efficiency and the power factor applying a boost AC-DC.

8. REFERENCES

[1] Y. Cheron, H. Foch and J. Salesses, "Study of a Resonant Converter Using Power Transistor in a 25-kW X-Ray Tube Power Supply," Proceedings of IEEE-PESC & Proceedings of European Space Power Application, pp. 295, June 1985.

[2] H. Hino, T. Hatakeyama, M. Nakaoka, "Resonant DC-DC Converter Using Parasitic Impedances of High-Voltage Transformer," Proceedings of PCIM-Europe Conference, Vol. 1, pp. 15, June 1987.

[3] A. K. S. Bhat, "Fixed-Frequency PWM Series-Parallel Resonant Converter," IEEE-Transactions of Industry Applications, Vol. 28, No. 5, pp. 1002, Sep.-Oct. 1992.

[4] H. Takano, H. Uemura, M. Nakaoka, "Advanced Constant-Frequency PWM Resonant DC-DC Converter with Real Time Digital Control for X-Ray Power Generator", Proceedings of EPE'91, Vol.1, pp. 544, Sep. 1991.

[5] H. Takano, J. Takahashi, T. Hatakeyama and M. Nakaoka, "Feasible Characteristic Evaluations of Resonant Tank PWM Inverter-Linked DC-DC High-Power Converters for Medical-Use High-Voltage Application," Proceedings of IEEE-APEC, Vol. 2, pp.913, March 1995.

[6] H. Takano, T. Hatakeyama, J. M. Sun, E. Hiraki and M. Nakaoka, "Digital controlled resonant PWM DC-DC converter based on 32-bit RISC processor," Proc. of JIASC, Vol. E, pp. 44-49, Aug. 1996.

[7] M. A. Perez, C. Blanco, M. Rico and F.F. Linera, "A New Topology for High Voltage, High Frequency Transformers," Proceedings of IEEE-APEC, Vol.2, pp. 554, March, 1995.

[8] Cecilio Blanco Viejo, Miguel Angel Perez Garcia, Manuel Rico Secades and Javier Uceda Antolin, "Improved high voltage, high frequency power supply : design criteria," EPE Journal, Vol.5, No. 2, Sep. 1995.

[9] V. Kaura and V. Blasko,"Operation of a Voltage Source Converter at Increased Utility Voltage," IEEE Trans. on PE, Vol.12, No.1, Jan. 1997.

[10] B. K. Bose," Power Electronics and AD Drives," Prentice-Hall Inc. 1986.